

Shape-dependent magnetic properties of low-dimensional nanoscale Prussian blue (PB) analogue $\text{SmFe}(\text{CN})_6 \cdot 4\text{H}_2\text{O}$ †

Hao-Ling Sun,^a Hongtao Shi,^b Fei Zhao,^a Limin Qi^{*b} and Song Gao^{*a}

Received (in Cambridge, UK) 23rd May 2005, Accepted 30th June 2005

First published as an Advance Article on the web 28th July 2005

DOI: 10.1039/b507240a

Unique nanorods and nanobelts of Prussian blue (PB) analogue $\text{SmFe}(\text{CN})_6 \cdot 4\text{H}_2\text{O}$ have been successfully synthesized by using reverse micelles as colloidal soft templates; magnetic studies show that the shape of the low-dimensional nanoscale material is a dominating factor for its coercivity due to the effect of shape anisotropy.

During the past decade, low-dimensional nanoscale materials, including nanotubes, nanorods, nanowires, and nanobelts, have attracted considerable attention due to their interesting physical properties and potential applications in nanodevices.^{1–5} Recently, keen efforts have been put into controlling the size and shape of nanomaterials and understanding the correlations between the physical properties and their size or shape. The magnetic properties of a material are very sensitive to its shape due to the dominating role of anisotropy in magnetism. The shape of magnetic materials is unequivocally one of the key factors governing their magnetic behavior.⁶

Prussian blue (PB) analogues $\text{M}_i^{m+}[\text{M}'(\text{CN})_6]^{n-}$ have played important roles in the field of molecular magnets due to the efficient ability of CN^- anion for transferring magnetic coupling.⁷ However, in general these bulky PB analogues have small coercivities, which prohibit their potential applications as hard magnets or high-density permanent information storage materials.⁸ One approach to increase the coercivity is to increase the energy barrier (E_A) for rotation of the magnetization orientation, which is called the anisotropy energy and its lowest order form is given by $E_A = KV \sin^2\theta$, where K is the anisotropy constant, V is volume of the nanoparticles and θ is the angle between the easy axis and magnetization direction.⁹ There are two ways to increase the anisotropy energy: (1) a chemical approach is choosing the anisotropic spin carriers so as to increase the contribution of the magneto-crystalline anisotropy constant (Co(II) being a favorite one for 3d transition metal ions and Sm(III) for lanthanide ions); (2) a physical means is altering the size and/or shape of the materials to increase the contribution of the surface or the shape anisotropy constant.¹⁰

Until now there are some reports about the size- or shape-dependent magnetic properties of nanoscale materials based on metals and metal oxides.⁶ However there are few reports about the size- or shape-dependent magnetic properties of nanoscale molecular magnets. During the past few years, Kitagawa and other groups reported their studies on the synthesis of PB nanoparticles and the size-dependent magnetic properties.^{11a–c} However, the shape-dependent magnetic properties of low-dimensional nanoscale PB are still rarely explored although some recent efforts have been devoted to the morphosynthesis of molecular magnetic materials.^{11d,e} Herein we report the shape-controlled synthesis of nanorods and nanobelts of PB analogues of $\text{SmFe}(\text{CN})_6 \cdot 4\text{H}_2\text{O}$ and their shape-dependent magnetic behavior.

Reverse micelles and microemulsions have been widely used as soft colloidal templates for controlling the size and/or shape of the nanoscale materials.¹² In particular, a variety of one-dimensional (1D) inorganic nanostructures such as BaCO_3 nanowires,^{12b} BaCrO_4 nanorods^{12c} and nanobelts^{12d} have been successfully synthesized in reverse micelle systems. It is noted that nanosized molecular magnets with a cubic morphology have been previously synthesized in anionic reverse micelles.^{12e,f} Recently, Prussian blue analogue $\text{Co}_3[\text{Co}(\text{CN})_6]_2$ nanostructures with morphologies of polyhedra, cubes and rods have been synthesized in a cationic microemulsion;^{12g} however, the shape-dependent magnetic properties of these nanostructures have not been explored. In this work, $\text{SmFe}(\text{CN})_6 \cdot 4\text{H}_2\text{O}$ nanocrystals with different shapes were synthesized by the reaction of $\text{K}_3\text{Fe}(\text{CN})_6$ and SmCl_3 solubilized in reverse micelles (supporting information†). Fig. 1 shows typical scanning electron microscopy (SEM) and transmission electron microscopy (TEM) images of $\text{SmFe}(\text{CN})_6 \cdot 4\text{H}_2\text{O}$ crystals obtained in aqueous solution and in reverse micelles formed by different surfactants. As shown in Fig. 1a, b, $\text{SmFe}(\text{CN})_6 \cdot 4\text{H}_2\text{O}$ microrods with diameters between 5–8 μm and aspect-ratios of about 10 were obtained in aqueous solution. The related X-ray diffraction (XRD) pattern (Fig. S1a†) indicates that the products were pure crystalline $\text{SmFe}(\text{CN})_6 \cdot 4\text{H}_2\text{O}$ with an orthorhombic unit cell (JCPDS card: 84–1954, $a = 0.7435 \text{ nm}$, $b = 1.2866 \text{ nm}$, $c = 1.3724 \text{ nm}$). In contrast, $\text{SmFe}(\text{CN})_6 \cdot 4\text{H}_2\text{O}$ nanorods with diameters typically ranging from 75 to 150 nm and aspect-ratios of about 20–30 were obtained in nonionic reverse micelles formed by polyoxyethylene (5) nonylphenyl ether (NP-5), cyclohexane, and water (Fig. 1c, d). The related XRD pattern (Fig. S1b†) demonstrated that the nanorods were also $\text{SmFe}(\text{CN})_6 \cdot 4\text{H}_2\text{O}$ crystals with the orthorhombic structure. Moreover, the electron diffraction (ED) pattern of the obtained $\text{SmFe}(\text{CN})_6 \cdot 4\text{H}_2\text{O}$ nanorods indicates that each nanorod was a single crystal grown along the a axis (Fig. 1d). It was expected that the orthorhombic $\text{SmFe}(\text{CN})_6 \cdot 4\text{H}_2\text{O}$ crystal

^aState Key Laboratory of Rare Earth Materials Chemistry and Applications & PKU-HKU Joint Laboratory on Rare Earth Materials and Bioinorganic Chemistry, College of Chemistry and Molecular Engineering, Peking University, Beijing 100871, P. R., China. E-mail: gaosong@pku.edu.cn

^bState Key Laboratory for Structural Chemistry of Unstable and Stable Species, College of Chemistry and Molecular Engineering, Peking University, Beijing 100871, China. E-mail: liminqi@pku.edu.cn

† Electronic supplementary information (ESI) available: Experimental details and Fig. S1–S4. See <http://dx.doi.org/10.1039/b507240a>

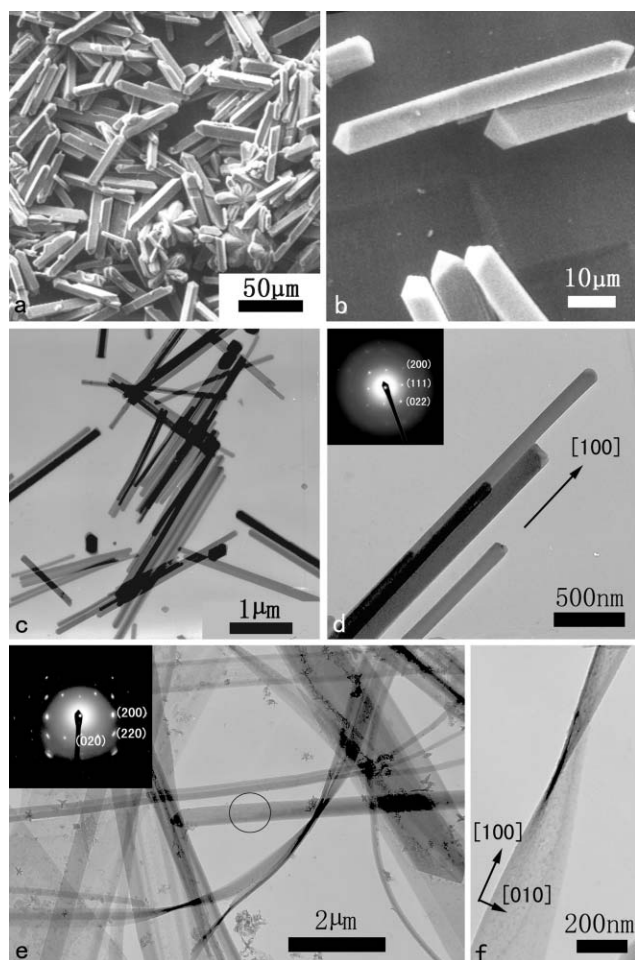


Fig. 1 SEM (a, b) and TEM (c–f) images of $\text{SmFe}(\text{CN})_6 \cdot 4\text{H}_2\text{O}$ crystals formed in aqueous solution (a, b), NP-5 reverse micelles (c, d) and CTAB–*n*-hexanol reverse micelles (e, f). Insets show the corresponding ED patterns.

with an *a* value much less than both the *b* and *c* values of its unit cell could have a tendency to grow into a rod-like morphology elongated along the *a* axis, leading to the formation of *a*-axis-oriented microrods in aqueous solution. When the reaction was carried out in aqueous nanodroplets of NP-5 reverse micelles, the crystal nucleation was limited inside the nanoreactors and the crystal growth was largely influenced by the interfacial surfactant film. The final formation of the high-aspect-ratio single-crystalline nanorods may result from the oriented aggregation of the primary nanoparticles, which is reminiscent of the formation of single-crystalline BaCO_3 nanowires in nonionic reverse micelles.^{12b}

When the synthesis was conducted in cationic reverse micelles formed by cetyltrimethylammonium bromide (CTAB), *n*-hexanol, cyclohexane and water, a dramatic change in the shape of the product was observed. Unique nanobelts with lengths up to several tens of micrometres, widths about 300 nm and thicknesses less than 20 nm were obtained (Fig. 1e, f). The related XRD pattern (Fig. S1c†) and energy-dispersive X-ray spectroscopy (EDS) spectrum (Fig. S2†) confirmed that the products were actually pure crystalline $\text{SmFe}(\text{CN})_6 \cdot 4\text{H}_2\text{O}$ with the orthorhombic structure. As shown in Fig. 1e, the ED pattern of a single nanobelt exhibited diffraction spots predominantly corresponding to the

[001] zone of the orthorhombic $\text{SmFe}(\text{CN})_6 \cdot 4\text{H}_2\text{O}$ with (*h*00) spots along the length direction, indicating that each nanobelt was a single crystal with the *a* axis along the length direction, the *b* axis along the width direction, and the *c* axis along the thickness direction. If an alcohol with a longer carbon chain was used to replace *n*-hexanol as the cosurfactant, the widths of the $\text{SmFe}(\text{CN})_6 \cdot 4\text{H}_2\text{O}$ nanobelts would be considerably decreased. For example, when *n*-decanol was used instead of *n*-hexanol, $\text{SmFe}(\text{CN})_6 \cdot 4\text{H}_2\text{O}$ nanobelts with widths about 40 nm were obtained (Fig. S3†). The exact formation mechanism of the belt-like structure remains unclear at the present time. However, it was speculated that with the aid of the cosurfactant of *n*-hexanol, the cationic surfactant CTAB could show specific interaction with the {001} faces of $\text{SmFe}(\text{CN})_6 \cdot 4\text{H}_2\text{O}$ crystals, leading to considerable limitation of the crystal growth along the [001] direction and the final formation of $\text{SmFe}(\text{CN})_6 \cdot 4\text{H}_2\text{O}$ nanobelts with the *c* axis along the thickness direction. Similarly, BaCrO_4 nanobelts were previously synthesized in reverse micelles formed by mixed cationic–anionic surfactants, where the interfacial films of mixed surfactants were believed to play an important role in the nanobelt formation.^{12d} To the best of our knowledge, this is the first solution synthesis of nanobelts of molecular magnets, which may provide a useful model system for the fundamental study of shape-dependent properties of magnetic nanomaterials based on molecular magnets. This synthetic strategy may open a new route to the facile morphology-controlled synthesis of low-dimensional nanostructures of molecular magnets.

The shape-dependent magnetic properties of these low-dimensional $\text{SmFe}(\text{CN})_6 \cdot 4\text{H}_2\text{O}$ nanoscale materials were studied by using an Oxford MagLab2000 system and a Quantum Design SQUID magnetometer. The zero field-cooled magnetization (ZFCM) and field-cooled magnetization (FCM) curves of the $\text{SmFe}(\text{CN})_6 \cdot 4\text{H}_2\text{O}$ microrods, nanorods, nanobelts and narrow nanobelts are shown in Fig. 2a. The peak temperatures (T_p) observed in the ZFCM curve of $\text{SmFe}(\text{CN})_6 \cdot 4\text{H}_2\text{O}$ nanorods, nanobelts and narrow nanobelts are obviously smaller than that of the $\text{SmFe}(\text{CN})_6 \cdot 4\text{H}_2\text{O}$ microrods (bulk), which is due to the size and/or surface effect of the nanomaterials.^{11a,13} A typical temperature dependence of $\chi_M T$ for the materials shows ferrimagnetic behavior (Fig. S4†), the same as reported.¹⁴ Interestingly, we found that the coercive field (H_c) of $\text{SmFe}(\text{CN})_6 \cdot 4\text{H}_2\text{O}$ nanorods, 2765 Oe, is obviously larger than the corresponding value of 785 Oe found in bulk $\text{SmFe}(\text{CN})_6 \cdot 4\text{H}_2\text{O}$ microrods (Fig. 2b). The coercivity is an extrinsic property of a magnet, which not only depends on the spin carrier but also on the shape or the size of the magnets. An increase in the coercivity of a magnetic material is considered to be due to an increase in the magnetic anisotropy since an applied field at a given temperature should be able to overcome the energy barrier and change the orientation of the magnetization. For a nonspherical piece of material, the total magnetic anisotropy can be expressed as $K = K_{\text{xtal}} + K_s$, where K_{xtal} represents the bulk magneto-crystalline anisotropy and K_s is the shape anisotropy.¹⁵ Shape anisotropy occurs in a system containing a nonspherical piece of material and makes it easier to induce magnetization along the long direction of the nonspherical material, since the demagnetizing field is less in the long direction due to the fact that the induced poles at the surface are further apart.⁹ Apparently, in a low-dimensional nanoscale system, shape

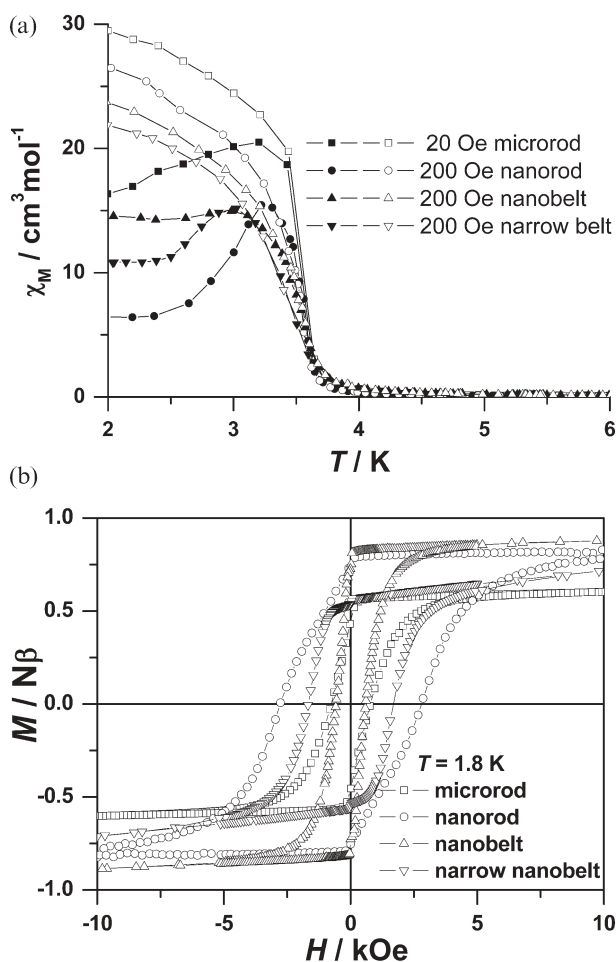


Fig. 2 Plots of field-cooled magnetization (FCM) and zero field-cooled magnetization (ZFCM) vs. temperature (a) and the hysteresis loops ($M/N\beta$ vs. H) measured at 1.8 K (b) for $\text{SmFe}(\text{CN})_6 \cdot 4\text{H}_2\text{O}$ microrods, nanorods, nanobelts and narrow nanobelts per SmFe unit.

anisotropy has a great effect on the magnitude of the coercive field (H_c). For $\text{SmFe}(\text{CN})_6 \cdot 4\text{H}_2\text{O}$ nanorods, it is not surprising that its H_c is larger than that of the $\text{SmFe}(\text{CN})_6 \cdot 4\text{H}_2\text{O}$ microrods (bulk) simply because of the shape anisotropy. The magnitude of the shape anisotropy is proportional to the length/diameter ratio, *ca.* 20–30 and 10 for the nanorods and microrods, respectively. The shape anisotropy constant (K_s) for the nanorods and microrods can be deduced from the equation $K_s = (N_a - N_c)M_s^2/2$, where N_a and N_c are demagnetization factors and M_s is the saturated magnetization. The value of $(N_a - N_c)$ is also estimated to be about 6.28 and 5.9 based on length/diameter ratio according to the published literature.⁹ The calculated shape anisotropy constants of nanorods and microrods are 2822 and 2651 erg cm^{-3} , respectively, which are qualitatively consistent with the order of their coercive fields. The H_c for $\text{SmFe}(\text{CN})_6 \cdot 4\text{H}_2\text{O}$ nanobelts and narrow belts are 600 and 1683 Oe, respectively. It is easy to understand the increase to the larger H_c for $\text{SmFe}(\text{CN})_6 \cdot 4\text{H}_2\text{O}$ narrow belts because the decrease of the width of the nanostructure will make the spins prefer to align along the long direction due to the increase in the demagnetizing field along the wide direction. Although the shape anisotropy plays an important role in the magnetic behavior

of the nanobelt, the H_c of $\text{SmFe}(\text{CN})_6 \cdot 4\text{H}_2\text{O}$ nanobelts is smaller than that of the bulk microrods probably because one of its dimensions is less than the single domain radius.

In conclusion, a variety of low-dimensional nanoscale Prussian blue analogue materials including unique $\text{SmFe}(\text{CN})_6 \cdot 4\text{H}_2\text{O}$ nanorods and nanobelts have been prepared by using reverse micelles as soft colloidal templates. The magnetic study of the obtained materials reveals that they exhibit interesting magnetic behavior, especially for their coercivities, which are dependent on the effect of shape anisotropy.

This work was supported by the National Science Fund for Distinguished Young Scholars (20125104, 20325312), NSFC no. 20221101, 20490210, and 20233010. We would like to thank Mr Zhao-Fei Li for helpful discussions on the X-ray diffraction and electron diffraction data.

Notes and references

- J. Hu, T. W. Odom and C. M. Lieber, *Acc. Chem. Res.*, 1999, **32**, 435.
- G. R. Patzke, F. K. Krumeich and R. Nesper, *Angew. Chem., Int. Ed.*, 2002, **41**, 2446.
- Y. Xia, P. Yang, Y. Sun, Y. Wu, B. Mayers, B. Gates, Y. Yin, F. Kim and H. Yan, *Adv. Mater.*, 2003, **15**, 353.
- C. N. R. Rao, F. L. Deepak, G. Gundiah and A. Govindaraj, *Prog. Solid State Chem.*, 2003, **31**, 5.
- Z. L. Wang, *Annu. Rev. Phys. Chem.*, 2004, **55**, 159.
- F. Dumestre, B. Chaudret, C. Amiens, M. Respaud, P. Fejes, P. Renaud and P. Zurcher, *Angew. Chem., Int. Ed.*, 2004, **43**, 1851; W. S. Seo, H. H. Jo, K. Lee, B. Kim, S. J. Oh and J. T. Park, *Angew. Chem., Int. Ed.*, 2004, **43**, 1115; R. D. Sanchez, J. Rivas, P. Vaquero, M. A. Lopez-Quintelad and D. Caeiro, *J. Magn. Magn. Mater.*, 2002, **247**, 92; Q. Song and Z. J. Zhang, *J. Am. Chem. Soc.*, 2004, **126**, 6164.
- S. Ohkoshi, Y. Abe, A. Fujishima and K. Hashimoto, *Phys. Rev. Lett.*, 1999, **82**, 1285; S. Ferlay, T. Mallah, R. Quahès, P. Veillet and M. Verdaguer, *Nature*, 1995, **378**, 701; H. S. Holmes and G. S. Girolami, *J. Am. Chem. Soc.*, 1999, **121**, 5593; S. Ohkoshi, T. Iyoda, A. Fujishima and K. Hashimoto, *Phys. Rev. B*, 1997, **56**, 11642; W. E. Buschmann, J. Enslin, P. Gutlich and J. S. Miller, *Chem. Eur. J.*, 1999, **5**, 3019; O. Sato, T. Iyoda, A. Fujishima and K. Hashimoto, *Science*, 1996, **272**, 704.
- H. Z. Kou, W. M. Bu, S. Gao, D. Z. Liao, Z. H. Jiang, S. P. Yan, Y. G. Fan and G. L. Wang, *J. Chem. Soc., Dalton Trans.*, 2000, 2996; H. Z. Kou, S. Gao, J. Zhang, G. H. Wen, G. Su, R. K. Zheng and X. X. Zhang, *J. Am. Chem. Soc.*, 2001, **123**, 11809.
- K. J. Klabunde, *Nanoscale Materials in Chemistry*, John Wiley & Sons, Inc, 2001, p. 195.
- A. Hutlova, D. Niznansky, J. L. Rehspringer, C. Estournes and M. Kurmoo, *Adv. Mater.*, 2003, **15**, 1622.
- (a) T. Uemura and S. Kitagawa, *J. Am. Chem. Soc.*, 2003, **125**, 7814; (b) L. Catala, T. Gacoin, J. P. Boilet, E. Revere, C. Paulsen, C. Lhotel and T. Mallah, *Adv. Mater.*, 2002, **15**, 826; (c) C. W. Ng, J. Ding, P. Y. Chow, L. M. Gan and C. H. Quek, *J. Appl. Phys.*, 2000, **87**, 6049; (d) P. Zhou, D. Xue, H. Luo and X. Chen, *Nano Lett.*, 2002, **2**, 845; (e) E. Dujardin and S. Mann, *Adv. Mater.*, 2004, **16**, 1125.
- (a) M. P. Pileni, *Nat. Mater.*, 2003, **2**, 145; (b) L. Qi, J. Ma, H. Cheng and Z. Zhao, *J. Phys. Chem. B*, 1997, **101**, 3460; (c) M. Li, H. Schnablegger and S. Mann, *Nature*, 1999, **402**, 393; (d) H. Shi, L. Qi, J. Ma, H. Cheng and B. Zhu, *Adv. Mater.*, 2003, **15**, 1647; (e) S. Vaucher, M. Li and S. Mann, *Angew. Chem., Int. Ed.*, 2000, **39**, 1793; (f) S. Vaucher, J. Fielden, M. Li, E. Dujardin and S. Mann, *Nano Lett.*, 2002, **2**, 225; (g) M. H. Cao, X. L. Wu, X. Y. He and C. W. Hu, *Chem. Commun.*, 2005, 2241.
- D. Michels, C. E. Krill III and R. Birringer, *J. Magn. Magn. Mater.*, 2002, **250**, 203.
- F. Hulliger, M. Landolt and H. Vetsch, *J. Solid State Chem.*, 1976, **18**, 283.
- J. S. Miller and M. Drillon, *Magnetism: Molecules to Materials III*, John Wiley & Sons, Inc, 2002, p. 230.